

Angular limitations of polymer-based waveguide holograms for 1-to-many V-shaped surface-normal optical interconnects

Maggie M. Li, Ray T. Chen, Suning Tang, and Dave Gerold

Microelectronics Research Center, Department of Electrical and Computer Engineering, University of Texas, Austin, Texas 78759

(Received 8 February 1994; accepted for publication 27 June 1994)

Experimental results of 1-to-2 intraplane and of 1-to-32 interplane V-shaped fanouts are delineated. Coupling efficiencies of 48% for surface-normal and of 45% for near-surface-normal interplane fanout beams are theoretically and experimentally confirmed. The influence of the angular fluctuation of a device having two multiplexed waveguide holograms with film thickness of $15\ \mu\text{m}$ and index modulation of 0.04 is studied. The angle between the two grating vectors is determined to be less than 26° to keep the near-surface-normal fanout beams.

Optical interconnects are of choice to replace conventional electrical interconnects in high-speed multiprocessor digital computers.¹⁻³ Recently, polymer-based integrated photonic circuit elements have been employed for a myriad of applications in optically interconnected systems due to their compatibility with various substrates and their low material dispersion. These system demonstrations include intraplane⁴⁻⁷ and interplane^{8,9} optical interconnects, and wavelength division (de)multiplexers.^{9,10} Very recently, two new 1-to-many three-dimensional (3D) board-to-board and backplane optical interconnect schemes were demonstrated using substrate guided waves.^{11,12} Intra- and interplane optical interconnects with parallel fanout beams and V-shaped fanout beams are important building blocks for intrawafer and chip-to-chip interconnects.⁴ For chip-to-chip optical interconnects, a V-shaped fanout pattern has the advantage of providing a straight optical path which reduces the loss of the optical bus significantly when compared with the conventional right-angle waveguide optical bus.¹³

In this letter, we present for the first time the theoretical analysis together with the experimental results of intra- and of interplane V-shaped 1-to-many optical interconnects. Two multiplexed waveguide holograms are employed to convert one surface normal incident beam into two intraplane substrate guided waves. The intraplane guided waves are then coupled with two hologram arrays integrated along the optical paths on intraplane beams to provide arrays of 1-to-2 inter-plane fanouts.

The schematic illustrating how the multiplexed waveguide holograms convert one surface normal incident beam into two substrate guided waves is shown in Fig. 1. The diffraction angle θ is greater than the critical angle θ_c of total internal reflection (TIR), i.e., $\theta \geq \theta_c$. The two holograms shown in Fig. 1 are recorded with the same diffraction angle which is 45° in our experiment. Different intraplane fanout directions are realized by rotating the recording plate an angle δ about its surface-normal axis. Each hologram was fabricated using the two-beam interference method.¹¹ In our experiment, we use an Argon laser operating at 488 nm as the recording beam, and a He-Ne laser as the reconstruction beam ($\lambda_r = 632.8\ \text{nm}$).

The photograph of the intraplane V-shaped 1-to-2 optical interconnects is shown in Fig. 2, where two substrate guided

waves are clearly displayed with $\delta = 15^\circ$. A He-Ne laser beam with transverse electric (TE) polarization was employed in the reconstruction. A coupling efficiency of 48% for each hologram was measured. For the intraplane optical interconnects shown in Fig. 2, by using substrate guided waves, a multiplexed hologram with linear dimension equivalent to that of the incident TEM₀₀ He-Ne laser beam is sufficient. This greatly reduces the surface area employed when compared with the conventional guided-wave devices.

For interplane optical interconnects, we need 2D arrays of a multiplexed hologram to convert intraplane substrate guided waves into interplane optical interconnect fanout beams. Figure 3(a) shows the phase-matching diagram of each multiplexed hologram containing two gratings which provide surface-normal (90°) and near-surface-normal (11° deviation from surface normal) fanouts. Note that the two grating vectors associated with each multiplexed hologram for intra- and interplane fanouts are formed with the same recording geometry.

A schematic of the interplane V-shaped optical interconnects demonstrated herein is shown in Fig. 3(b) where the far field V-shaped fanouts resulting from the 2D hologram arrays are illustrated. Each intraplane fanout beam on the master plate is coupled with two gratings associated with the multiplexed hologram arrays along the zig-zag optical paths. Two interplane fanout beams are generated each time when

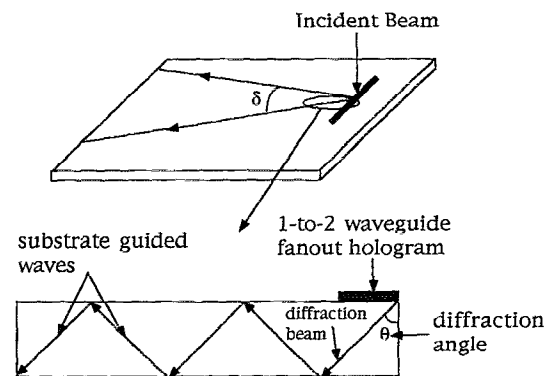


FIG. 1. Schematic of the demonstrated 1-to-2 intraplane interconnects with a surface-normal incident beam.



FIG. 2. The photograph of the V-shaped intraplane optical interconnects.

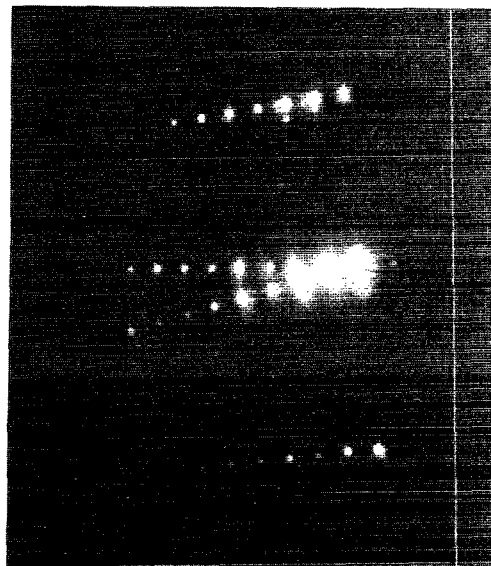
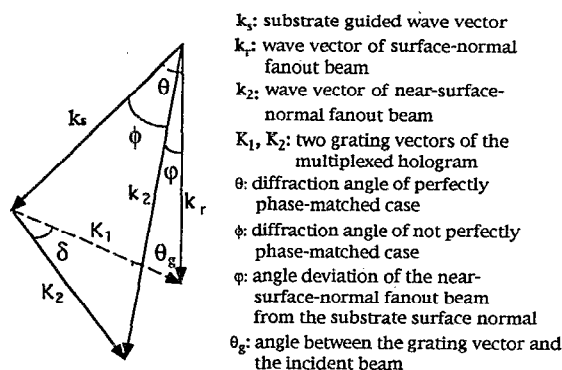
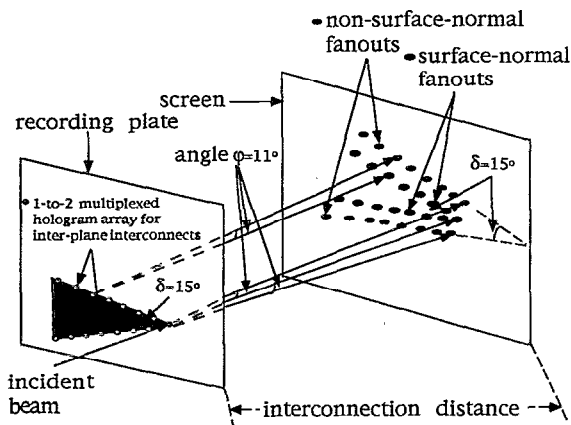


FIG. 4. The photograph of the V-shaped 1-to-32 interplane fanouts.



(a)



(b)

FIG. 3. (a) Phase-matching diagram within the substrate for surface-normal and near-surface-normal fanout beams. (b) The schematic of interplane V-shaped 1-to-many optical interconnects.

the intraplane guided wave comes across a multiplexed hologram. One beam results from the coupling between the substrate guided wave vector k_s and the grating vector K_1 of one hologram. This represents the perfectly phase-matched case. The fanout beam is normal to the substrate surface. The other beam is activated due to the interaction between the substrate guided wave vector k_s and the grating vector K_2 of the other hologram. This is designed to provide near-surface normal with a deviation angle of 11° which is not perfectly phase matched in our case.

Figure 4 shows the photograph of an interplane V-shaped 1-to-many optical interconnects consisting of the 2D multiplexed hologram arrays with $\delta=15^\circ$. It shows the far field pattern of 1-to-32 inter-plane fanouts containing 16 surface-normal and 16 near-surface-normal beams.

To understand the influence of the angles δ and φ on the grating coupling efficiency of the near-surface-normal fanouts for interplane optical interconnects, the coupling efficiencies of the surface-normal fanout beam (η_0) and of the near-surface-normal fanout beam (η) were further studied using coupled wave theory.¹⁴ For the substrate guided mode, the interplane fanout hologram is a transmission hologram. The coupling efficiency η is¹⁴

$$\eta = \sin^2(v^2 + \xi^2)^{1/2} / (1 + \xi^2/v^2), \quad (1)$$

where

$$v = \pi \Delta n d / \lambda_r (c_r c_s)^{1/2}, \quad (2)$$

$$\xi = \Delta \psi K d \sin(\theta - \psi_0) / 2 c_s = -\Delta \lambda K^2 d / 8 \pi n c_s, \quad (3)$$

$$c_r = \cos \psi_0, \quad c_s = \cos \psi_0 - (K/k_r) \cos \theta_g. \quad (4)$$

In above equations, Δn is the modulation of the refractive index of the holographic film, d is the thickness of the film, ψ_0 is the incident angle, $\Delta \psi$ is the deviation of the incident angle, θ_g is the angle between the grating vector and the incident beam [see Fig. 3(a)], and K is the magnitude of the grating vector \mathbf{K} .

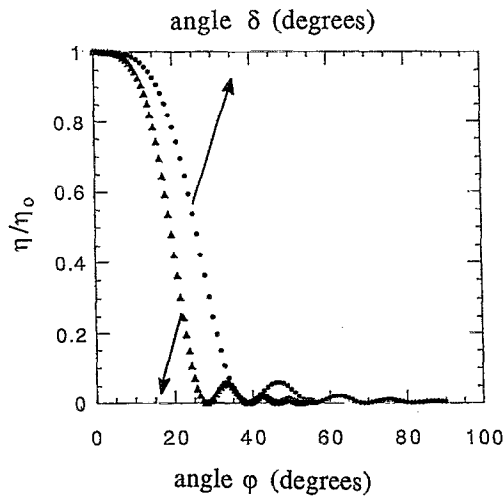


FIG. 5. Normalized coupling efficiency (η/η_0) of the near-surface-normal fanout beams as functions of angles δ and ϕ .

For the perfectly phase-matched case, i.e., the surface-normal fanouts, $\Delta\psi=0$. For the near-surface-normal case $\Delta\psi=\phi-45^\circ$ where ϕ is the diffraction angle which is not perfectly phase matched [see Fig. 3(a)]. We use η to represent the near-surface-normal coupling efficiency and ϕ to represent the deviation angle of the near-surface-normal beam from the surface-normal beam. From Fig. 3(a) the expressions for ϕ and φ can be derived as

$$\cos \phi = (k_r^2 + k_2^2 - K^2) / 2k_r k_2, \quad (5)$$

$$\cos \varphi = \{k_r^2 + k_2^2 - [2K \sin(\delta/2)]^2\} / 2k_r k_2, \quad (6)$$

$$k_2 = [K^2 + k_r^2 - 2k_r K \cos \delta \sin(\theta/2)]^{1/2}, \quad (7)$$

where $\lambda_r=632.8$ nm, $\Delta n=0.04$, $d=15$ μm , $\psi_0=0^\circ$, $\theta=45^\circ$, $\theta_g=67.5^\circ$, and $n=1.512$ are chosen in our experiment. Using these parameters, we have $\eta_0=51.3\%$ using Eq. (1) with $\xi=0$. The calculated result of η/η_0 with different δ and φ is shown in Fig. 5. It is clear that when $\delta=15^\circ$ and $\varphi=11^\circ$, which is equivalent to our experiments, we have $\eta/\eta_0=0.926$, therefore $\eta=47.5\%$. To eliminate or to keep the near-surface-normal fanouts, appropriate ranges of δ and of φ have to be chosen when designing the device. From Fig. 5 we know that for our parameters, δ should be bigger than 30° to eliminate the near-surface-normal fanout beam, while δ

should be less than 26° and φ should be less than 16° if the near-surface-normal fanout beams are desired.

The measured coupling efficiencies for our device are 48% for the surface-normal fanout beam and 45% for the near-surface-normal fanout. A good agreement between our experimental results and theoretical analysis is found.

In summary, we report the theoretical analysis and the experimental results for a novel intraplane and interplane V-shaped 1-to-many optical interconnect that uses a 2D multiplexed waveguide hologram array and substrate guided waves. 1-to-2 intraplane optical interconnect fanouts and 1-to-32 inter-plane fanouts containing 16 surface-normal and 16 near-surface-normal beams are delineated. We further measured the coupling efficiencies for the surface-normal and the near-surface-normal interplane fanout beams. Excellent agreement between the measured results and our theoretical analysis is obtained. The influence of the angles δ and φ on coupling efficiency of the near-surface-normal beam is detailed and appropriate design criteria for δ and for φ are provided.

This research is currently sponsored by AFOSR, BMDO the Center of Optoelectronics Science and Technology (COST), and CRAY Research Inc.

- ¹J. W. Goodman, F. I. Leonberger, S. Kung, and R. A. Athale, Proc. IEEE **72**, 850 (1984).
- ²M. R. Feldman, S. C. Esener, C. C. Guest, and S. H. Lee, Appl. Opt. **27**, 1742 (1988).
- ³R. T. Chen, *Critical Rev. of Opt. Sci. and Tech.*, edited by K. K. Wang and M. Razeghi (SPIE, Los Angeles, 1993), Vol. CR45, p. 198.
- ⁴R. T. Chen, H. Lu, D. Robinson, M. Wang, G. Savant, and T. Jansson, J. Lightwave Technol. **10**, 888 (1992).
- ⁵R. T. Chen, M. R. Wang, and T. Jansson, Appl. Phys. Lett. **57**, 2071 (1990).
- ⁶M. R. Wang, G. J. Sonek, R. T. Chen, and T. Jansson, Appl. Opt. **31**, 236 (1992).
- ⁷R. Volkel, M. Heissmeier, H. Kobolla, U. Krackhardt, S. Rosner, J. Schmidt, J. Schwider, J. T. Sheridan, N. Streibl, and F. Zobel, SPIE **1849**, 104 (1993).
- ⁸R. T. Chen, H. Lu, D. Robinson, Z. Sun, and T. Jansson, Appl. Phys. Lett. **60**, 536 (1992).
- ⁹R. T. Chen, H. Lu, D. Robinson, and T. Jansson, Appl. Phys. Lett. **59**, 1144 (1991).
- ¹⁰V. Miniér and J. M. Xu, Opt. Eng. **32**, 2054 (1993).
- ¹¹R. T. Chen, S. Tang, M. M. Li, D. Gerold, and S. Natarajan, Appl. Phys. Lett. **63**, 1883 (1993).
- ¹²S. Tang and R. T. Chen, OSA/IEEE Integrated Photonics Research, 1994 Technical Digest Series 3, p. 277 (1994).
- ¹³R. T. Chen, Final Report to Army Space and Strategic Defense Command, Contract No. DASG60-90-C-0018 (1992).
- ¹⁴H. Kogelnik, Bell Sys. Tech. J. **48**, 2909 (1969).